Nitrogen–inversion in some aziridine type compounds: Structural and kinetic investigations by ab initio methods

ARTICLE *in* JOURNAL OF MOLECULAR STRUCTURE THEOCHEM · JANUARY 2001

Impact Factor: 1.37 · DOI: 10.1016/S0166-1280(00)00583-2

3 AUTHORS, INCLUDING:

Farzad Deyhimi
Shahid Beheshti University
79 PUBLICATIONS **667** CITATIONS
SEE PROFILE

Hossein Roohi
University of Guilan
74 PUBLICATIONS **427** CITATIONS
SEE PROFILE

ELSEVIER

Journal of Molecular Structure (Theochem) 535 (2001) 247–256

THEO CHEM

www.elsevier.nl/locate/theochem

Nitrogen-inversion in some aziridine type compounds: structural and kinetic investigations by ab initio methods

A. Ebrahimi[a], F. Deyhimi[b,*], H. Roohi[a]

[a]*Department of Chemistry, Sistan and Balouchestan University, Zahedan, Iran*
[b]*Department of Chemistry, Shahid Beheshti University, Evin-Tehran 19839, Iran*

Received 20 December 1999; revised 16 April 2000; accepted 8 May 2000

Abstract

Using ab initio HF molecular orbital and hybrid HF-density functional (B3LYP) methods, molecular structure of various nitrogen containing three-membered ring compounds, in their ground and planar-shaped transition states, corresponding to nitrogen-inversion process, were determined. For the nitrogen-inversion process in these compounds, the energy, enthalpy and free energy changes along with the activation barrier energy, the conventional Arrhenius parameters and the rate constants were also determined. The results predict that the increasing inversion energy barrier, due to the presence of highly electronegative atom into the three-membered ring or substituted adjacent to nitrogen (out-of-ring), e.g. a halogen or an alkoxy group, should allow the isolation of the resulted optically active chiral nitrogen center compounds. © 2001 Elsevier Science B.V. All rights reserved.

Keywords: Nitrogen-inversion; Ab initio methods; Transition states; Optical activity; Kinetic parameters

1. Introduction

The relatively low energy barrier to pyramidal nitrogen-inversion in trivalent amines does not permit its detection on the time scale of the NMR spectrometer. At room temperature, this energy barrier is 6–7 kcal/mol in trivalent amines [1,2]. The influence of angle strain and electronic effects on these inversion barriers were the subject of many experimental works e.g. [2–8]. In aziridine compounds, the incorporation of the nitrogen atom into a three-membered ring causes the energy barrier of N-inversion to increase to 18–20 kcal/mol [2].

The addition of a highly electronegative atom adjacent to nitrogen (e.g. a halogen or an alkoxy group) increases this energy barrier even more, so that the isolation of the resultant optically active chiral nitrogen compounds become possible [3–6].

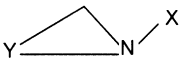

X : H, CH_3, OCH_3, Cl, Ph

Y : CH_2 , O, S, NH

In *N*-chloro-2,2-diphenylaziridine [6], a barrier energy of 24.4 kcal/mol was obtained for the nitrogen-inversion energy, based on the kinetics calculations of the racemization rate. The synthesis of some optically active diaziridines have also been reported in literature, where the $\Delta G^{\#}$ of racemization was determined by NMR to be in the range 27–28 kcal/mol [2].

* Corresponding author. Tel.: +98-21-240-1765; fax: +98-21-240-3041.

E-mail address: f.deyhimi@cc.sbu.ac.ir (F. Deyhimi).

PII: S0166-1280(00)00583-2

Similarly, the experimental values for N-inversion in oxaziridines compounds having carbon, nitrogen and oxygen atoms in a three-membered ring were also reported to be in the range 24–31 kcal/mol [7,8]. In this work the nitrogen inversion in various aziridine type compounds having carbon, nitrogen, oxygen or sulfur atoms into the three-membered ring and also different substituted out-of-ring atom adjacent to nitrogen, has been studied by ab initio molecular orbital and hybrid HF-density functional (B3LYP) methods. The rate of racemization for the compounds, which are capable of existing as enantiomers, has also been calculated.

2. Computational methods

Ab initio calculations and geometry optimizations were carried out for all the above mentioned aziridine compounds with the GAUSSIAN 98 [9] program package using the standard 6-31G(d,p) basis set [10] with HF and hybrid HF-density functional (B3LYP) methods [11,12]. Vibrational analysis was also performed at these levels in order to confirm the nature of stationary species and to provide the harmonic frequencies needed in the computation of thermodynamic and kinetic parameters. The nature of the stationary points has been fixed for all these compounds by virtue of the number of imaginary frequencies at these levels. For the minimum state structure, only the real frequency values and in the planar-shaped transition state structure only one imaginary frequency value was accepted. For the reaction of racemization, the rate constants have been calculated using the conventional transition state theory, whose results can be formally rewritten using the following pseudo-thermodynamic functions [13–15]:

$$\begin{aligned} \mathrm{k}(T) &= \chi(T)\frac{\mathrm{k}T}{\mathrm{h}}\exp\left(\frac{-\Delta G^{\#}}{\mathrm{R}T}\right) \\ &= \chi(T)\frac{\mathrm{k}T}{\mathrm{h}}\exp\left(\frac{\Delta S^{\#}}{\mathrm{R}}\right)\exp\left(\frac{-\Delta H^{\#}}{\mathrm{R}T}\right) \\ &= A\exp\left(\frac{-E_{\mathrm{a}}}{\mathrm{R}T}\right) \end{aligned} \quad (1)$$

where k is the Boltzmann constant, h is the Planck constant, $\Delta H^{\#}$, $\Delta G^{\#}$ and $\Delta S^{\#}$ are the enthalpy, Gibbs free energy and entropy changes between initial (reactants) and transition state structures, respectively, R is the ideal gas constant, A is the so-called pre-exponential factor, and E_{a} represents the activation energy. The transmission coefficient $\chi(T)$ accounts for the re-crossing and tunneling effects, although it is generally represented by a unitary value in the basic theory [14].

3. Results and discussion

3.1. Geometrical structure

Using HF and HF-density functional methods (B3LYP), the structural geometrical parameters of the above-mentioned aziridine type compounds in the equilibrium state and planar-shaped transition state (TS) structures were determined, where the results are reported in Tables 1 and 2. For the TS structures, the corresponding imaginary frequencies in N-inversion are also included in these tables. The results show that for these aziridine type compounds, in the quasi-pyramidal form, the angle values calculated by the HF method are usually larger than those calculated by B3LYP method (0.08–2.36°). Inversely, in TS quasi-planar structure, the B3LYP angle and bond length values are larger than those obtained by the HF method (0–1.66° and 0–7.5%, respectively).

The results in Table 2 show further that, in the planar-shaped transition state, the increase in all bond angle values are accompanied by a decrease in bond lengths (except for the N–Y bond length in compound **17**). The CNY strained angle increases generally more in compound with a high electronegative group X (e.g. an alkoxy or Cl group such as in compounds **13**, **14**, **11**, **16**, **18**, and **19**) compared to the case where both X and Y are highly electronegative. The variation of CNY angle value lie in the range 3.96–10.47°, corresponding, respectively, to compounds **7** and **13**. Conversely, the resulting decrease in bond lengths vary in the range −0.02 to −0.19 Å. The lowest changes observed in bond length are: −0.02 Å (for N–Y in compounds **12** and **17**), −0.04 Å (for N–C in compound **23**) and −0.02 Å

Table 1
Calculated geometric parameters of different aziridine type compounds, their planar-shaped transition state structures (TS) and imaginary frequencies, for N-inversion calculated by the HF method. Bond lengths are in angstrom units, angles in degrees and (*) is used for *cis* structure

X, Y	Bond angle (°)			Torsion angle (°)	Bond length (Å)			ω
	CNY	YNX	CNX	XNCY	N–Y	N–C	N–X	
1 H, CH_2	61.10	111.70	111.69	103.58	1.448	1.448	1.001	
(TS)	65.87	147.08	147.08	179.87	1.390	1.390	0.984	998.96
2 H, O	57.48	104.49	109.43	95.14	1.445	1.408	1.005	
(TS)	60.92	129.34	169.76	−179.96	1.423	1.351	0.980	1349.44
3 H, S	66.88	107.73	110.85	101.05	1.778	1.417	1.003	
(TS)	72.03	141.59	146.40	179.88	1.704	1.372	0.984	1083.84
4 H, NH	59.28	106.01	110.88	−96.69	1.453	1.422	1.002	
(TS)	63.99	138.42	157.41	174.06	1.412	1.363	0.982	1209.97
5 H, NH*	59.15	110.05	109.89	102.05	1.459	1.424	1.004	
6 CH_3, CH_2	61.83	117.26	117.26	107.96	1.438	1.438	1.445	
(TS)	66.08	146.45	147.48	179.58	1.389	1.389	1.421	410.61
7 CH_3, O	57.96	109.44	115.84	97.64	1.442	1.399	1.450	
(TS)	60.89	129.93	169.16	−179.69	1.428	1.351	1.413	573.93
8 CH_3, S	67.39	115.06	116.35	107.81	1.773	1.408	1.455	
(TS)	72.04	141.32	146.66	180.00	1.706	1.369	1.426	448.41
9 CH_3, NH	59.88	111.26	116.51	−100.32	1.446	1.414	1.449	
(TS)	64.27	138.19	157.52	177.28	1.410	1.360	1.416	508.31
10 CH_3, NH*	60.02	115.13	116.35	105.16	1.449	1.414	1.446	
11 OCH_3, CH_2	61.36	110.18	110.18	102.60	1.446	1.446	1.397	
(TS)	68.70	145.65	145.66	−179.22	1.374	1.374	1.349	509.91
12 OCH_3, O	58.60	112.51	118.07	100.53	1.421	1.404	1.365	
(TS)	62.80	132.09	165.07	175.86	1.414	1.345	1.321	772.74
13 OCH_3, S	66.37	111.93	108.86	106.34	1.803	1.410	1.374	
(TS)	74.26	142.65	143.09	178.73	1.688	1.364	1.342	559.99
14 OCH_3, NH	59.79	108.75	109.35	−100.95	1.442	1.417	1.381	
(TS)	66.76	138.49	154.65	175.39	1.393	1.351	1.337	670.90
15 OCH_3, NH*	59.73	109.80	107.83	102.95	1.448	1.419	1.389	
16 Cl, CH_2	61.05	114.52	114.52	105.60	1.451	1.451	1.730	
(TS)	67.36	146.32	146.32	−179.94	1.383	1.383	1.655	459.48
17 Cl, O	58.32	109.80	112.81	99.92	1.411	1.413	1.737	
(TS)	62.03	132.00	165.98	179.99	1.410	1.355	1.629	641.73
18 Cl, S	66.99	115.24	113.71	108.64	1.761	1.426	1.733	
(TS)	73.09	143.88	143.06	179.94	1.692	1.373	1.652	484.59
19 Cl, NH	59.66	111.16	114.50	101.12	1.430	1.427	1.733	
(TS)	65.38	139.32	155.24	−176.41	1.399	1.361	1.641	571.04
20 Cl, NH*	59.42	113.13	111.98	104.68	1.438	1.433	1.747	
21 Ph, CH_2	61.91	121.03	121.03	111.15	1.437	1.437	1.408	
(TS)	65.74	147.15	147.15	179.99	1.393	1.393	1.363	292.60
22 Ph, O	57.83	112.20	116.57	100.64	1.435	1.407	1.430	
(TS)	61.56	132.17	166.27	−179.99	1.409	1.355	1.359	464.67
23 Ph, S	67.40	119.32	119.28	112.00	1.767	1.412	1.420	
(TS)	71.81	143.19	145.01	−179.92	1.700	1.378	1.370	328.10
24 Ph, NH	59.76	114.53	118.04	103.51	1.441	1.420	1.425	
(TS)	64.17	139.28	156.41	−174.53	1.404	1.366	1.358	389.24

(for N–X in compounds **1** and **3**) and the resulting highest length variation values are: −0.16 Å (for N–Y bond in compound **13**), −0.14 Å (for N–C bond in compound **21**) and −0.16 Å (for N–X bond in compound **17**). The XNCY torsion angle lies in the range: 94.24 (in compound **2**) to 110.97° (in compound **21**), where the lowest observed variation of the torsion angle in planarization (from the

Table 2
Calculated geometric parameters of different aziridine type compounds, their planar-shaped transition state structures (TS) and imaginary frequencies, for N-inversion calculated by the B3LYP method. Bond lengths are in angstrom units, angles in degrees and (*) is used for the *cis* structure

X, Y	Bond angle (°)			Torsion angle (°)	Bond length (Å)			ω
	CNY	YNX	CNX	XNCY	N–Y	N–C	N–X	
1 H, CH_2	60.58	109.69	109.69	102.06	1.473	1.473	1.019	
(TS)	66.22	146.89	146.89	179.95	1.400	1.400	0.999	895.44
2 H, O	56.86	102.65	106.98	94.24	1.498	1.440	1.028	
(TS)	60.89	129.30	169.47	−179.91	1.424	1.352	0.981	1349.44
3 H, S	66.07	105.08	108.38	98.77	1.833	1.440	1.023	
(TS)	72.70	140.66	146.66	180.00	1.738	1.377	0.999	1014.54
4 H, NH	58.75	103.59	108.51	−94.97	1.503	1.449	1.022	
(TS)	64.92	138.24	156.73	175.59	1.440	1.372	0.997	1100.07
5 H, NH*	58.74	108.36	107.75	101.10	1.451	1.451	1.025	
6 CH_3, CH_2	61.72	116.02	116.02	106.86	1.460	1.460	1.457	
(TS)	66.37	146.19	147.41	179.94	1.400	1.400	1.423	370.00
7 CH_3, O	57.20	108.28	113.97	97.00	1.502	1.430	1.465	
(TS)	61.16	130.56	168.32	179.98	1.475	1.364	1.409	532.61
8 CH_3, S	66.52	113.44	114.60	106.14	1.831	1.428	1.467	
(TS)	72.48	140.44	147.06	−180.00	1.745	1.376	1.424	423.23
9 CH_3, NH	59.43	109.67	114.81	−99.07	1.495	1.438	1.464	
(TS)	65.13	138.13	156.75	179.66	1.438	1.371	1.415	463.15
10 CH_3, NH*	59.78	113.99	114.80	104.44	1.492	1.438	1.460	
11 OCH_3, CH_2	60.58	108.24	108.24	101.09	1.473	1.473	1.450	
(TS)	69.21	145.43	145.36	−178.23	1.387	1.387	1.380	450.85
12 OCH_3, O	57.24	111.88	117.05	99.74	1.499	1.440	1.401	
(TS)	62.62	133.67	163.55	173.56	1.478	1.361	1.332	706.03
13 OCH_3, S	64.01	111.41	107.26	105.89	1.901	1.436	1.401	
(TS)	74.48	142.03	143.44	177.37	1.741	1.372	1.361	533.83
14 OCH_3, NH	58.85	107.26	107.36	−100.04	1.502	1.446	1.427	
(TS)	67.76	139.01	153.11	175.78	1.427	1.365	1.359	601.78
15 OCH_3, NH*	58.94	108.76	105.57	102.81	1.503	1.448	1.441	
16 Cl, CH_2	60.33	112.42	112.42	103.86	1.478	1.478	1.796	
(TS)	68.59	145.71	145.71	−179.97	1.390	1.390	1.695	429.18
17 Cl, O	58.39	109.52	109.82	101.27	1.438	1.450	1.838	
(TS)	62.59	133.25	164.14	−179.97	1.459	1.368	1.646	626.58
18 Cl, S	66.34	114.13	110.69	108.16	1.807	1.452	1.823	
(TS)	74.15	143.09	142.78	179.96	1.730	1.377	1.679	485.57
19 Cl, NH	59.25	109.64	112.24	100.33	1.467	1.458	1.813	
(TS)	67.04	139.42	153.54	−178.25	1.424	1.370	1.670	546.07
20 Cl, NH*	59.12	112.05	108.40	−105.18	1.455	1.472	1.852	
21 Ph, CH_2	61.83	120.88	120.88	110.97	1.456	1.546	1.412	
(TS)	65.91	147.05	147.05	179.98	1.406	1.406	1.369	256.27
22 Ph, O	56.99	111.11	115.16	99.76	1.497	1.440	1.441	
(TS)	61.93	132.93	165.12	−179.99	1.449	1.371	1.359	422.38
23 Ph, S	66.61	118.15	118.21	110.56	1.823	1.429	1.425	
(TS)	72.31	142.13	145.57	−179.97	1.737	1.385	1.371	313.37
24 Ph, NH	59.35	113.19	117.12	102.17	1.487	1.446	1.433	
(TS)	64.88	139.23	155.85	−176.95	1.432	1.38	1.362	348.20

Table 3
Calculated ab initio energy values (HF and B3LYP methods), ln(k) and Arrhenius parameters for N-inversion process. (a): Arrhenius parameters determined by graphical method and (b) by formula (see text). The reported energy values are in kJ/mol and ($*$) is used for the *cis* structure

X, Y	$\Delta E^{\#}$		$\Delta H^{\#}$		$\Delta G^{\#}$		ln(k) (s^{-1})		E_a		A (10^{13} s^{-1})	
	HF	DFT	HF	DFT	HF	DFT	HF	DFT	(a)	(b)	(a)	(b)
1 H, CH_2	72.23	66.80	72.09	66.57	72.30	66.92	0.48	3.04	67.12	69.05	1.20	1.47
2 H, O	141.96	140.56	141.99	140.61	141.93	140.55	−27.56	−26.22	140.06	143.09	1.41	1.74
3 H, S	90.18	92.15	90.08	90.05	90.25	92.24	−6.75	−7.06	92.21	94.53	1.23	1.56
4 H, NH	125.41	118.77	125.37	118.69	125.42	118.81	−20.92	−17.69	118.64	121.17	1.26	1.61
5 H, NH*	99.51	95.30	99.43	95.15	99.55	95.39	−12.79	−8.24	95.08	97.63	1.20	1.53
6 CH_3, CH_2	74.68	66.64	74.93	66.80	72.16	63.73	0.43	3.88	68.77	69.28	5.39	5.84
7 CH_3, O	144.59	139.15	144.72	139.13	143.78	138.43	−28.43	−26.14	140.66	141.61	1.95	2.24
8 CH_3, S	89.66	89.56	89.82	89.56	88.12	88.31	−6.00	−6.01	91.39	92.03	2.54	2.80
9 CH_3, NH	127.33	115.78	127.41	115.71	126.30	114.85	−21.39	−16.68	117.43	118.18	2.13	2.39
10 CH_3, NH*	103.43	97.60	103.61	97.67	102.26	96.46	−11.70	−9.26	99.39	100.15	2.45	2.75
11 OCH_3, CH	146.97	129.60	148.10	130.62	145.09	127.68	−28.97	−21.87	132.51	133.10	5.20	5.52
12 OCH_3, O	222.96	216.70	222.76	216.54	223.10	216.31	−60.39	−57.41	217.54	219.01	1.52	1.85
13 OCH_3, S	171.54	172.31	170.95	171.64	171.84	172.69	−39.76	−39.96	173.16	174.12	0.96	1.11
14 OCH_3, NH	218.40	199.37	217.96	198.80	218.70	199.73	−58.64	−50.81	200.10	201.27	0.98	1.16
15 OCH_3, NH	207.51	191.92	206.68	191.10	208.31	192.73	−54.45	−47.99	192.38	193.58	0.73	0.88
16 Cl, CH_2	107.92	105.02	107.19	104.05	108.07	105.36	−14.05	−12.88	105.80	106.53	0.88	1.00
17 Cl, O	203.61	218.87	203.25	218.10	205.56	219.26	−52.53	−58.63	219.28	220.58	0.90	1.10
18 Cl, S	121.42	138.46	120.78	137.45	121.48	138.83	−19.45	−26.34	139.05	139.93	0.84	0.97
19 Cl, NH	173.55	174.48	173.06	173.66	173.56	174.75	−40.45	−40.78	175.08	176.13	0.92	1.09
20 Cl, NH*	155.69	165.03	155.12	163.94	155.74	165.49	−35.56	−37.05	165.33	166.42	0.75	0.90
21 Ph, CH_2	44.50	35.43	43.65	34.43	45.51	36.69	11.16	14.72	36.67	36.91	0.66	0.68
22 Ph, O	112.02	98.28	111.55	97.79	113.44	99.68	−16.22	−10.59	99.67	100.27	0.73	0.79
23 Ph, S	70.53	51.86	54.60	51.06	56.83	53.15	6.60	8.11	53.20	53.54	0.67	0.73
24 Ph, NH	91.52	74.88	90.85	74.15	93.26	76.52	−8.09	−1.30	76.21	76.63	0.62	0.65

equilibrium to the planar-shaped transition state) is 69.01° (in compound **21**) and the highest variation is 85.67° (in compound **2**).

3.2. N-inversion—kinetic aspects

The calculated $\Delta E^{\#}$, $\Delta H^{\#}$ and $\Delta G^{\#}$ energy barrier values for the pyramidal N-inversion are reported in Table 3. $\Delta E^{\#}$ values represent, each time, the difference between the corrected zero-point energy (ZPE) of the planar-shaped transition state and the initial quasi-pyramidal structure in its lowest energy state. The results reported in Table 3 also show that in these aziridine type compounds, the electronegativity of both the Y and X groups influence significantly the magnitude of the inversion barrier energy. For a given Y group (incorporated into the ring), the inversion barrier energy increases in the following order under the influence of X:

$$\begin{aligned}
&Y = O: && (X = Cl) > (X = O) > (X = CH_3) > (X = H) > (X = Ph);\\
&Y = S: && (X = Cl) > (X = H) > (X = CH_3) > (X = Ph);\\
&Y = N: && (X = H) > (X = CH_3) > (X = Ph);\\
&Y = CH_2: && (X = CH_3) > (X = H) > (X = Ph).
\end{aligned}$$

Similarly, for a given (out-of-ring) X group, the inversion barrier energy increases as following under the influence of Y:

$$\begin{aligned}
&X = Cl: && (Y = O) > (Y = NH) > (Y = S) > (Y = CH_2) > (Y = Ph);\\
&X = OCH_3: && (Y = O) > (Y = NH) > (Y = S) > (Y = CH_2).
\end{aligned}$$

Thus, the more electronegative X and Y are, the

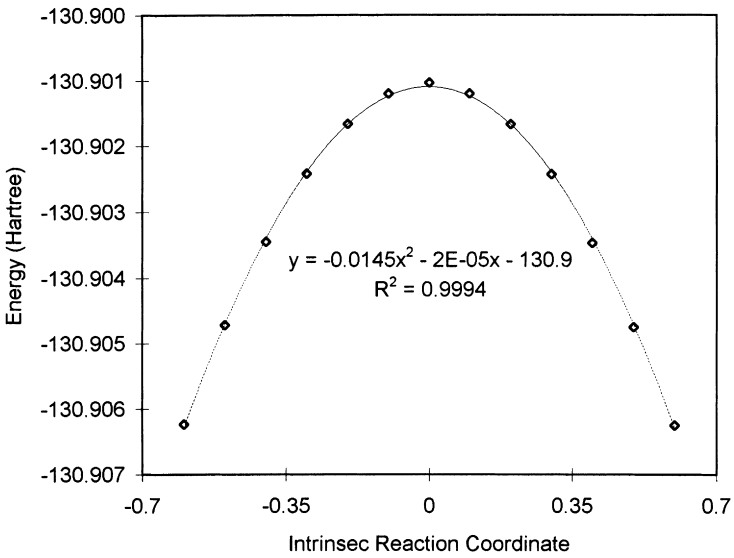

Fig. 1. Calculated ab initio potential energy values (B3LYP data) versus intrinsic reaction coordinate for compound **1**.

greater is the energy barrier to nitrogen inversion in these aziridine type compounds. For the majority of these compounds, with activation energy value greater than 97 kJ/mol [2], the results suggest that the corresponding invertomers could be isolated.

An evaluation of the tunneling effect is provided by the Wigner expression, which gives a temperature-dependent relation for the transmission coefficient in terms of the single imaginary frequency (ω) of the transition structure (see Tables 1 and 2)

$$\chi(T) = 1 + \frac{1}{24}\left(\frac{\mathrm{h}\omega}{\mathrm{k}T}\right)^2 \tag{2}$$

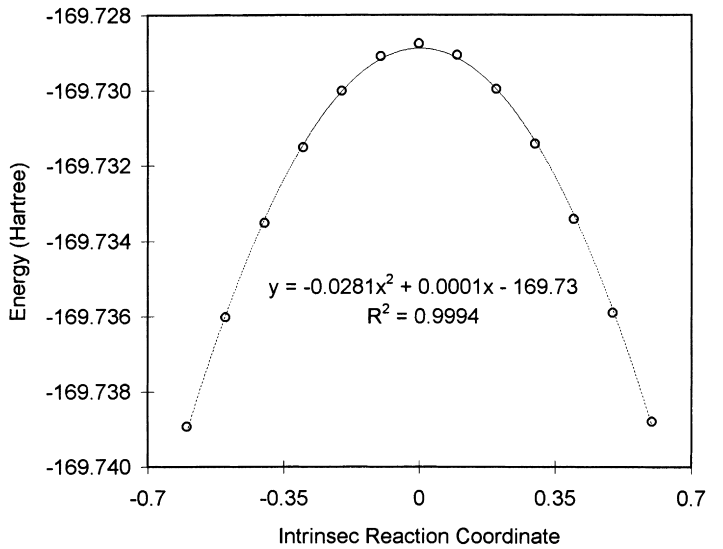

Fig. 2. Calculated ab initio potential energy values (B3LYP data) versus intrinsic reaction coordinate for compound **2**.

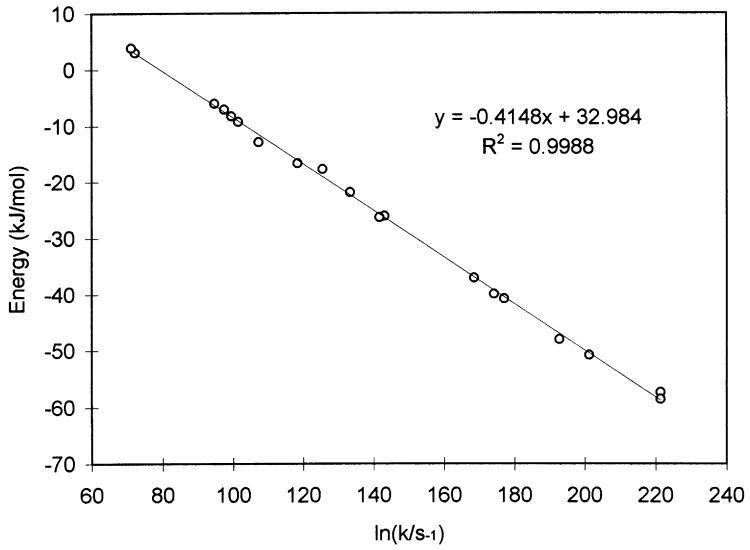

Fig. 3. Linear correlation between potential energy ΔE ($= \Delta E^{\#} - \Delta$ZPE) and ln(k) using B3LYP data.

The calculated transmission coefficients vary in the ranges: $1.06 \leq \chi(298\ \mathrm{K}) \leq 1.27$ and $1.06 \leq \chi(298\ \mathrm{K}) \leq 2.77$, respectively, for the single imaginary frequency value (ω) of the transition structures obtained by HF and B3LYP methods. At low temperatures, the effect of tunneling could significantly be increased and more refined model is required to compute reliable rate constants in these conditions [16,17].

As the magnitude of the N-inversion activation energy is relatively high in these compounds, the difference between the conventional and variational location of the transition structure must be comparatively insignificant. Using B3LYP data, this fact has

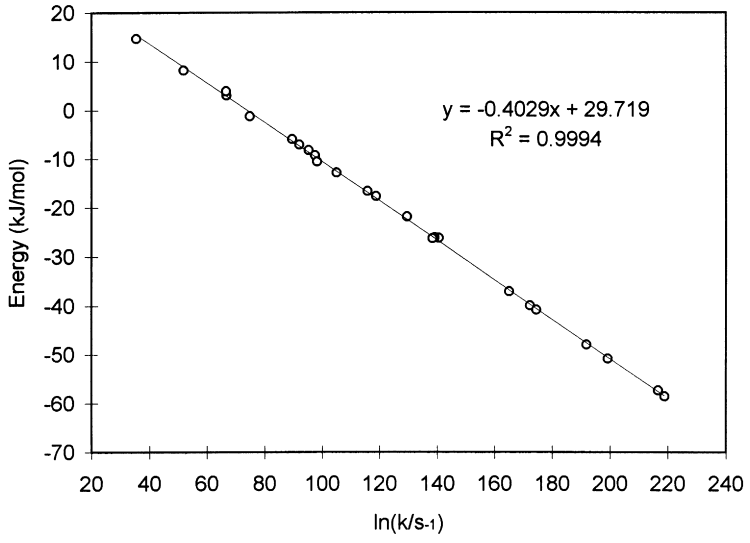

Fig. 4. Linear correlation between potential energy $\Delta E^{\#}$ and ln(k) using B3LYP data.

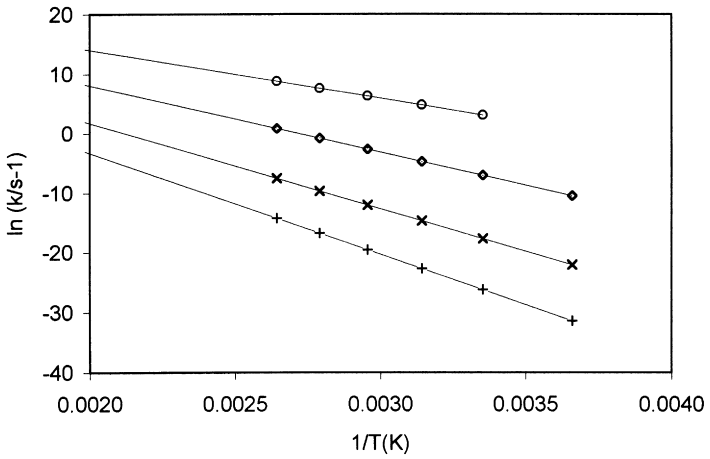

Fig. 5. Activation energy for N-inversion versus ln(k) (Arrhenius plot), for the aziridine type compounds: **1** (○), **2** (+), **3** (◇) and **4** (×).

been checked by plotting separately the potential energy ΔE ($= \Delta E^{\#} - \Delta$ZPE) versus the intrinsic reaction coordinate (IRC) for the two representative compounds (**1** and **2**). The resulting curves are given in Figs. 1 and 2. For the points near the TS, the evaluation of the ZPE and free energies show that the location of conventional and variational transition structures are effectively very close in both cases. Using B3LYP data, the canonical rate constants were also calculated at 298 K (see Table 3). As shown in Figs. 3 and 4, linear correlation (with $R^2 = 0.9988$ and 0.9994, respectively) are found for $\Delta E^{\#}$ and ΔE, both versus the ln(k), by the B3LYP method. This fact indicates that the rate of inversion is essentially affected by the magnitude of the potential energy rather than by the other parameters such as ZPE or entropy (which both could play only a minor role). The Arrhenius parameters were also calculated by two different procedures (a and b), using B3LYP data (see Table 3). In the first procedure (a), ln(k) was calculated at different temperature (in the range 270–380 K) and the results were then plotted versus 1/T. The Arrhenius parameters were then evaluated graphically from the slope ($-E_a$/R) and the intercept

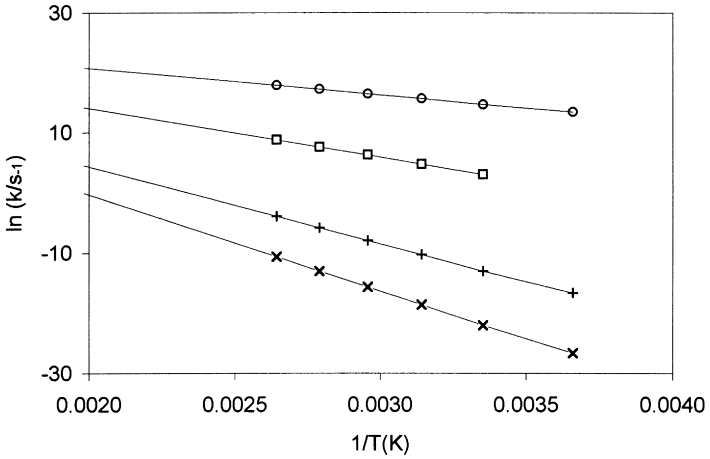

Fig. 6. Activation energy for N-inversion versus ln(k) (Arrhenius plot), for the aziridine type compounds: **6** (□), **11** (×) and **16** (+), **21** (○).

(ln(A)) of these plots. Figs. 5 and 6 show the linearity resulting in the representative Arrhenius plots for some of these aziridine type compounds. In the second procedure (b), the Arrhenius parameters were calculated based on the following relations: $E_a = \Delta H^{\#} + RT$ and $A = (kTe/h)\exp(\Delta S^{\#}/R)$. All the calculated results obtained by these two methods are included in Table 3. The variation between the E_a values obtained by these two methods lie in the range 0.5–3%.

Whether or not the 6-31G(d,p) basis set used in this investigation would lead to wrong results has also been checked. Actually this standard basis set could be critical for nitrogen as lacking orbital d-functions. The Massage keyword in GAUSSIAN 98, giving the possibility to add additional uncontracted basis functions to a standard basis set, was used to add 6D (or 7F) shells to non-hydrogen atoms and P (or 6D) shells to hydrogen atoms. For the aziridine molecules ($X \neq OCH_3$ or $X \neq Ph$), studied in this work, the modifications of $\Delta E^{\#}$ obtained by this adjustment were found to be in the range 0.5–1.2%. In addition, the use of 6-311++G(d,p) basis set for these aziridine molecules ($X \neq OCH_3$ or $X \neq Ph$), produced also a $\Delta E^{\#}$ change in the range 1–2.5%. The effect of the solvent on the modification of barrier heights has also been examined for the aziridine molecules ($X \neq OCH_3$ or $X \neq Ph$) by SCRF keyword (Onsager model). The presence of the solvents, with dielectric constants lying in the range 2–80, resulted in a ±1.5–3.5% change compared to the isolated molecules in the gas phase.

4. Conclusions

The structural geometrical parameters of the above mentioned aziridine type compounds in equilibrium state and planar-shaped transition state (TS) structures, as well as the corresponding imaginary frequencies and kinetics parameters for nitrogen inversion were determined using HF and HF-density functional methods (B3LYP). In the studied aziridine compounds, in which the nitrogen atom is incorporated into a three-membered ring, the results show quantitatively how the presence of the substituted X and Y groups could increase the relatively low energy barrier to pyramidal nitrogen inversion. This barrier energy, which is 20.92–29.29 kJ/mol in trivalent amines at room temperature [1,2], is increased up to 220 kJ/mol (for X = Cl and Y = O, compound **17**). Generally, the more electronegative X and Y are, the greater is the energy barrier to nitrogen inversion in these aziridine type compounds. The results suggest also that the isolation of the majority of these optically active aziridine compounds (with Y = O, S or NH but $Y \neq CH_2$), which have their energy barrier to N-inversion $E_a \geq 97$ kJ/mol (at room temperature), should be possible. The addition of a highly electronegative atom adjacent to nitrogen (e.g. a halogen or an alkoxy group) also increases more the variation of the strained CNY angle on planarization (up to 10.47° for compound **13**). Generally, in planarization, the increase of the bond angles is accompanied by a decrease in bond lengths. The quality of the linear correlations, found between ln(k) and the activation inversion barrier energy as well as $1/T$, supports the reliability of the calculated energetic and kinetics parameters.

References

[1] K.B.G. Torssell, Nitrile oxides, Organic Nitro Chemistry Series, VCH, New York, 1988.
[2] F.A. Davis, R.J. Jenkins Jr., Asymmetric Synthesis, vol. 4, Academic Press, New York, 1983 (chap. 4).
[3] S.J. Boris, J. Am. Chem. Soc. 90 (1968) 506.
[4] R. Gree, R. Carrie, J. Am. Chem. Soc. 99 (1977) 6667.
[5] R. Annunziata, R. Fornasier, F. Montanari, J. Chem. Soc. Chem. Commun. (1971) 1133.
[6] A. Forni, I. Moretti, A.V. Proxianky, G. Torre, J. Chem. Soc. Chem. Commun. (1981) 588.
[7] J. Bjorgo, D.R. Boyd, J. Chem. Soc. Perkin Trans. 2 (1973) 1575.
[8] A. Forni, G. Garuti, I. Moretti, G. Torre, G.D. Bocelli, P. Sgarabotto, J. Chem. Soc. Perkin Trans. (1978) 401.
[9] M.J. Frisch, G.W. Trucks, H.B. Schlegel, G.E. Scuseria, M.A. Robb, J.R. Cheeseman, V.G. Zakrzewski, J.A. Montgomery, Jr., R.E. Stratmann, J.C. Burant, S. Dapprich, J.M. Millam, A.D. Daniels, K.N. Kudin, M.C. Strain, O. Farkas, J. Tomasi, V. Barone, M. Cossi, R. Cammi, B. Mennucci, C. Pomelli, C. Adamo, S. Clifford, J. Ochterski, G.A. Peterson, P.Y. Ayala, Q. Cui, K. Morokuma, D.K. Malick, A.D. Rabuck, K. Raghavachari, J.B. Foresman, J. Cioslowski, J.V. Ortiz, B.B. Stefanov, G. Liu, A. Liashenko, P. Piskorz, I. Komaromi, R. Gomperts, R.L. Martin, D.J. Fox, T. Keith, M.A. Al-Laham, C.Y. Peng, A. Nanayakkara, C. Gonzalez, M. Challacombe, P.M.W. Gill, B. Johnson, W. Chen, M.W. Wong, J.L. Andres, M. Head-Gordon, E.S. Replogle, J. A. Pople, GAUSSIAN 98, Gaussian Inc., Pittsburgh PA, 1998.

[10] M.M. Francl, W.J. Pietro, W.J. Hehre, J.S. Binkley, M.S. Gordon, D.J. DeFrees, J.A. Pople, J. Chem. Phys. 77 (1982) 3654.
[11] A.D. Becke, J. Chem. Phys. 98 (1993) 1372.
[12] C. Lee, W. Yang, R.G. Parr, Phys. Rev. B 37 (1988) 785.
[13] R. Arnaud, R. Subra, V. Barone, F. Lelj, S. Olivella, A. Sole, N. Russo, J. Chem. Soc. Perkin Trans. 2 (1986) 1517.
[14] R. Arnaud, N. Bugaud, V. Vetere, V. Barone, J. Am. Chem. Soc. 120 (1998) 5733.
[15] M.J. Pilling, P.W. Seakins, Reaction Kinetics, Oxford University Press, Oxford, UK, 1995.
[16] D.G. Truhlar, J. Chem. Soc. Faraday Trans. 2 (1994) 1740.
[17] C. Minichino, V. Barone, J. Chem. Phys. 100 (1994) 3717.